Effect of microstructure on fatigue crack propagation in a titanium-aluminide alloy under thermomechanical fatigue conditions

- Current activities in the subcommittee of Titanium-Aluminide alloys in the Society of Materials Science, Japan (JSMS) -

Yasuhiro Yamazaki [a *], Ryota Sugaya [b], Fumio Tooyama [b]

[a] *Department of Mechanical Engineering*
[b] *Graduate School of Science and Engineering, Chiba University, Chiba*
[c] *Interdisciplinary Faculty of Science and Engineering, Shimane University, Matsue, Japan*
[*] *y.yamazaki@chiba-u.jp*

Titanium aluminide (TiAl) alloys have attracted to considerable interest as a material of blade in the low-pressure turbine section of aero engines since their superior specific strength. The mechanical properties and strengths of TiAl alloys are strongly sensitive to their microstructure controlled with thermo-mechanical processing. The collaborative research has been started from 2017 by the subcommittee on Titanium-Aluminide alloys, JSMS Committee on High Temperature Strength of Materials, in order to get basic information about the influence of microstructure on the high-temperature strength. This paper is a part of the collaborative research. The crack propagation tests were carried out under the load controlled out-of-phase type TMF (OP-TMF) loading condition with temperature range 400 ℃-760 ℃. The effect of microstructure on fatigue crack propagation behavior in was discussed.

1. Introduction

Titanium aluminide (TiAl) alloys have a high specific strength to creep and fatigue due to their low density, and oxidation resistance, and high melting temperature [1-10]. Particularly in the temperature range of 600–800 °C, TiAl alloys exhibit similar or better specific strength as compared with currently used Ni-base superalloys. Therefore, they alloys have attracted to considerable interest as a material of blade in the low-pressure turbine section of aero engines [1-3]. The mechanical properties and strengths of TiAl alloys are strongly sensitive to their microstructure controlled with thermo-mechanical processing [5-10]. The collaborative research has been started from 2017 by the subcommittee on Titanium-Aluminide alloys, JSMS Committee on High Temperature Strength of Materials, in order to get basic information about the influence of microstructure on the high-temperature strength. This project covers strength in creep, high-temperature fatigue, creep-fatigue, thermo-mechanical fatigue, fretting fatigue, and crack propagation, targeting a TiAl alloy prepared by unified thermo-mechanical histories. The members of the subcommittee are listed in Table 1. This paper deals with the effect of microstructure on the fatigue crack propagation behavior under the out-of-phase type TMF condition performed as a part of the collaborative research.

2. Experimental procedures

The material tested in this study is a forged titanium aluminide alloy with a chemical composition (in at.%) 43 Al, 5V, 4Nb, and Ti balance. The microstructures of the tested materials are shown in Fig. 1, and the results of the EBSD analysis are shown in Fig.2 Two materials with the different microstructure (denoted by NL, TL) were prepared by controlling the heat-treatment after the high-temperature forging. The NL specimen has the near α_2/γ-lamellar microstructure. The β-phase is present along the grain boundaries of lamellar-colonies. The TL specimen has a higher containing of β-phase. The microstructure of the TL specimen consists of α_2/γ lamellar colonies, equiaxed γ grains, and β-grains.

The center notched plate specimens with a width of 14 mm and a thickness of 2mm were used to study crack propagation behavior. Before the fatigue crack propagation test, the fatigue pre-crack with a total length of approximately 3 mm was introduced from the mechanical center notch at room temperature. The surfaces of all specimens were mechanically polished to mirror smoothness using alumina powders before and after the crack propagation tests. The observations and measurements of crack growth behavior were conducted by using a laser microscope after cooling to room temperature.

The crack propagation tests were carried out under the load controlled out-of-phase type TMF (OP-TMF) loading condition with temperature range 400℃-760 ℃. The test conditions are summarized in Table 2. During the crack propagation test,

the crack opening displacement was measured by using a extensometer with a gage length of 5 mm attached across the mechanical notch.

Table 1 The member of the subcommittee on Titanium-Aluminide alloys, JSMS

Affiliation	Member	Experimental item
Chiba Univ.	Y. Yamazaki (Chairman)	Crack propagation (TMF, LCF)
Iwate Univ.	H. Waki (Secretary)	Elastic anisotropy
IHI	Y. Ohta (Secretary), K, Kubushiro, Y. Sakakibara	Basic properties, Microstructure
Fukui Univ.	T. Hiyoshi (Secretary)	Creep (Multiaxial)
Ritsumeikan Univ.	T. Itoh, F. Ogawa	Fatigue, Creep (Multiaxial)
Shounan Int. of Tech.	T. Ohtani	Nondestructive damage evaluation
Kagoshima Univ.	K. Komazaki	Small sample testing technique
Tokyo Inst. of Tech.	M. Sakaguchi	Fatigue crack propagation
Shibaura Inst. of Tech.	S. Hashimura	Fretting wear
Nagaoka Univ. of Tech.	Y. Miyashita, T. Honma, M. Okazaki	Fretting fatigue, Microstructure
Niigata Inst. of Tech.	S. Yamagishi	High temp. deformation
Ohita Univ.	T. Yamamoto	Fatigue, Creep (Multiaxial)
Kiguchi Technics	R. Tagami, W. Fujiki	Fatigue
Kobe Mat. Testing Lab.	H. Hattori, K. Nakai, M. Nkatani	Fatigue
Ebara	Y. Hayabusa, R. Takakuwa	Creep
Shimane Univ.	F. Tooyama	Microstructure
Honda R&D, HRD Sakura	T. Munemura, T. sMiyashita	Coating
MHI	H. Kaneko, T. Karato	

Table 2 Conditions of fatigue crack propagation tests

Type	Out-of-phase (load control)
Temperature (Min. and Max.)	400 - 760 ℃
Laod range (stress range)	7500 N (268 MPa)
Load ratio (stress ratio)	-0.5
Loading wave form	Triangle
Frequency	1/360 Hz
Phase angle between load and temperature	-180 deg.

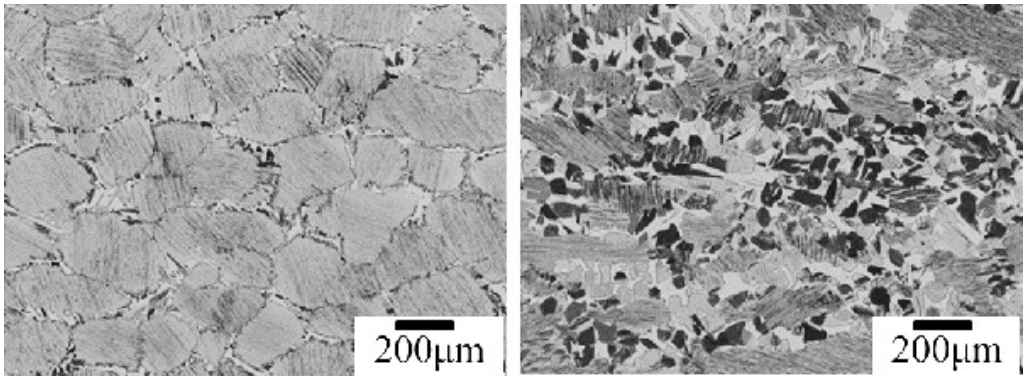

(a) NL specimen (b) TL specimen

Fig. 1 Microstructures of the tested materials.

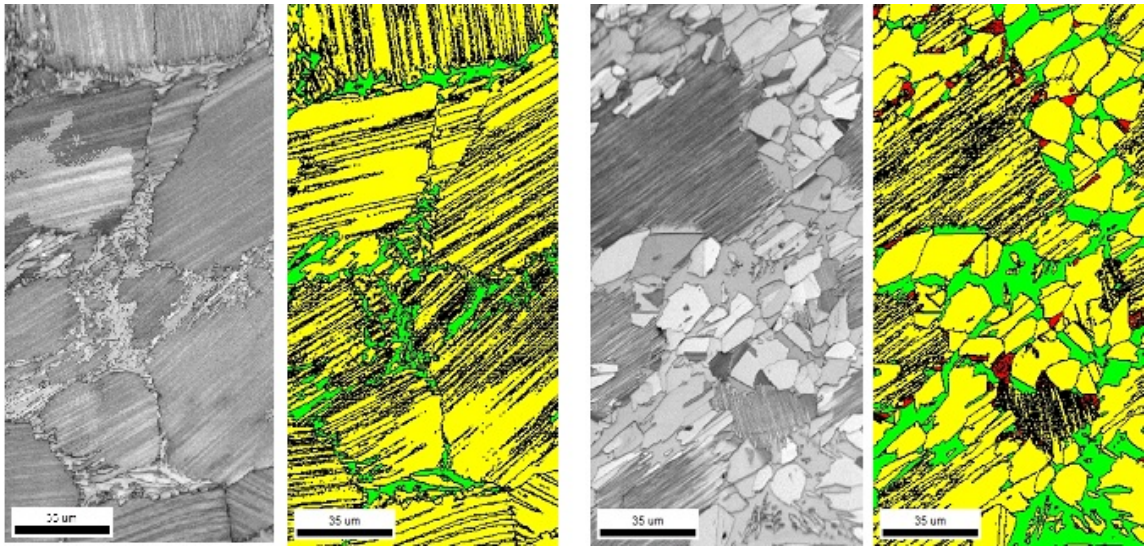

(a) Image quality and Phase maps of NL specimen (b) Image quality and Phase maps of TL specimen

Fig. 2 Results of EBSD analysis of the tested materials; Red: α-phase, Green: β-phase, Yellow: γ-phase.

3. Results and Discussions

Typical loading stress - crack opening displacement (COD) curve is shown in Fig. 3. The crack opening displacement, δ was evaluated from the measured displacement during propagation test minus the thermal expansion which was measured during the temperature cycle without loading before the test. The crack closure was evaluated by the compliance method with the loading stress - COD curve. The crack opening ratio, $U = \Delta K_{eff}/\Delta K$ was evaluated by following equation with the crack closure stress, σ_{cl}.

$$U = (\sigma_{max} - \sigma_{cl})/(\sigma_{max} - \sigma_{min}) \quad (1)$$

Where, σ_{max} and σ_{min} are the maximum stress and minimum stress of a loading cycle. Figure 4 shows the evaluated crack opening ratios, U correlated with the half crack length normalized by the half specimen width. As shown in Fig. 4, the values of U are almost independent to the crack length and material.

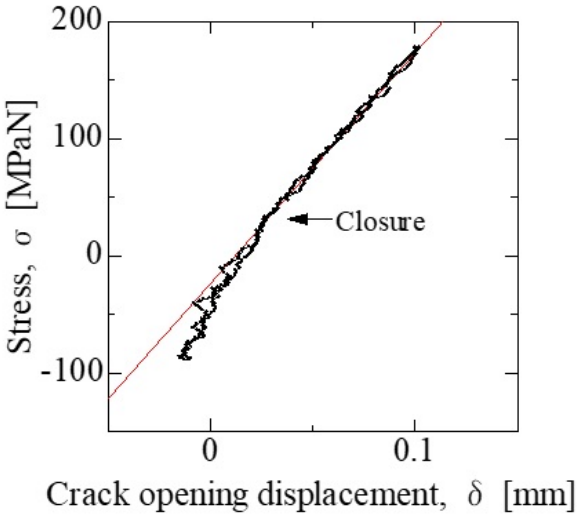

Fig. 3 Typical loading stress - crack opening displacement (COD) curve.

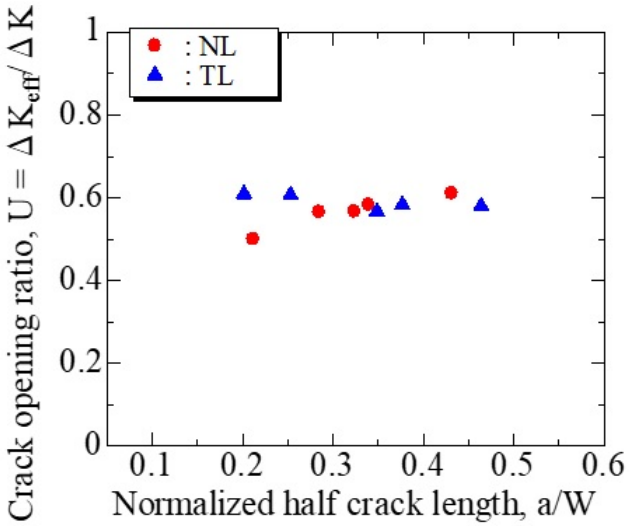

Fig. 4 Crack opening ratio correlated with the normalized half crack length.

Figure 5 shows the fatigue crack propagation rates under the out-of-phase type TMF (OP-TMF) condition correlated with the effective stress intensity factor, ΔK_{eff}. The ΔK_{eff} was evaluated as follows.

$$\Delta K_{eff} = U\Delta\sigma\sqrt{\pi a}F \qquad \text{with} \quad F = \sqrt{1/cos\,(\pi a/w)} \tag{2}$$

Where, $\Delta\sigma$ is the stress range, a is the half crack length, W is the half specimen width, respectively. In Fig. 5, the fatigue crack propagation curves, that were obtained under the iso-thermal high cycle fatigue (IHCF) condition at the minimum and the maximum temperatures of the TMF test [11], are also shown to comparison. As shown in Fig. 5, the fatigue crack propagation rates under the OP-TMF condition are remarkably higher than not only those under the IHCF one at 400℃ but also those under the IHCF one at 760℃. The high cycle fatigue crack propagation tests were conducted by using the CT specimen at T = 400℃ or 760℃, f = 10Hz, R_σ = 0.4. It can be considered that the fatigue crack propagation of the OP-TMF might be accelerated by the oxidation effect, the effect of creep damage related to the low loading rate, and so on. The further investigation should be performed in our collaborative research.

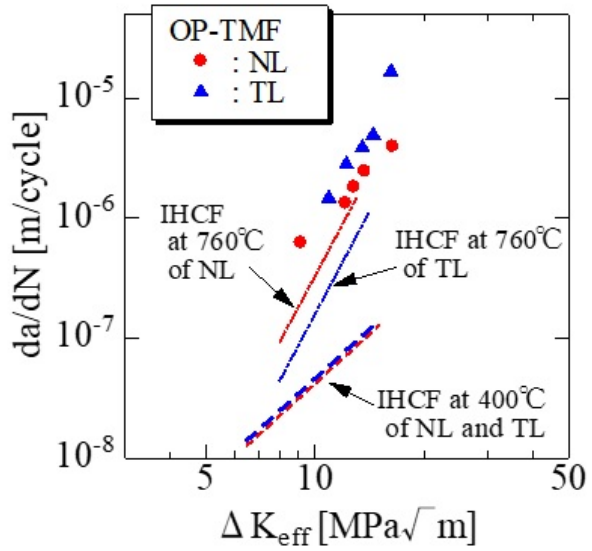

Fig. 5 Fatigue crack propagation rates correlated with the effective stress intensity factor, ΔK_{eff}.

In Fig. 5, the NL specimen exhibits higher resistance to fatigue crack propagation under the OP-TMF condition. From a microscopic viewpoint, the fatigue crack propagation behavior was also strongly affected by microstructure, such as lamellar structures and grain boundaries. Typical macroscopic crack propagation behaviors are shown in Fig. 6. Macroscopically, the fatigue cracks propagated perpendicularly to the loading axis. However, in the NL specimen, the crack propagation is strongly affected by the microstructure. In the NL specimen, the main fatigue crack propagated with

the branching and kinking. On the other hand, in TL specimen, the crack propagated almost straight perpendicular to the loading axis independent to microstructure. The fracture surfaces are shown in Fig. 7 and 8. As shown in Fig. 7, the crack plane of the NL specimen represents the rough surface depending with the microstructure. On the other hand, that of the TL specimen is almost flat (Fig. 8). The EBSD analysis were performed around crack path. The results for the NL and TL specimens are shown in Fig. 9 and Fig. 10, respectivery. In the NL specimen, the fatigue crack propagated along the interface of lamellar and the boundaries of the lamellar colonies. On the other hand, as shown in Fig. 10, the fatigue crack propagated across the lamellar colonies in the TL specimen. It can be concluded from these results that the driving force for crack propagation in the NL specimen is decreased due to the branching and kinking of main crack affected by microstructure.

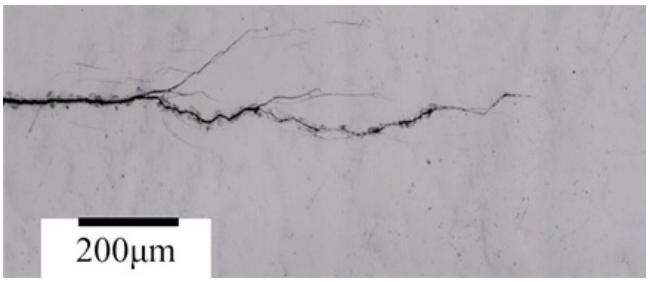

(a) NL specimen

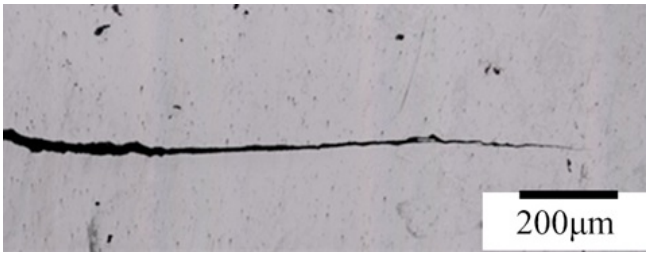

(b) TL specimen

Fig. 6 Crack propagation morphologies on the specimen surface.

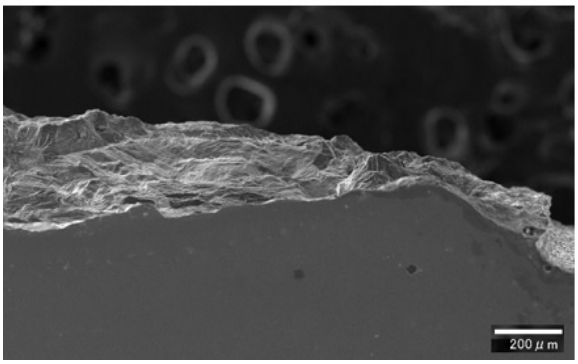

(a) macroscopic view

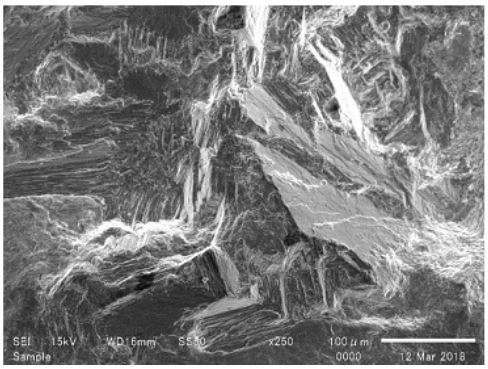

(b) Enlarged view

Fig. 7 Fracture surface of the TL specimen after the test.

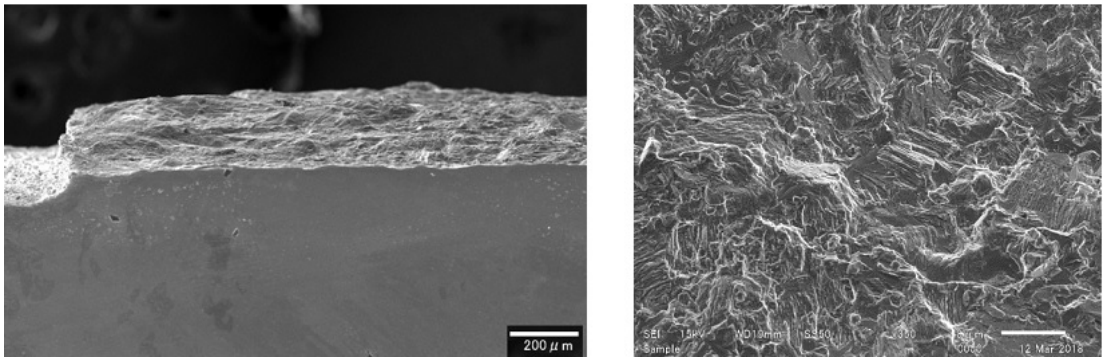

(a) macroscopic view (b) Enlarged view

Fig. 8 Fracture surface of the TL specimen after the test.

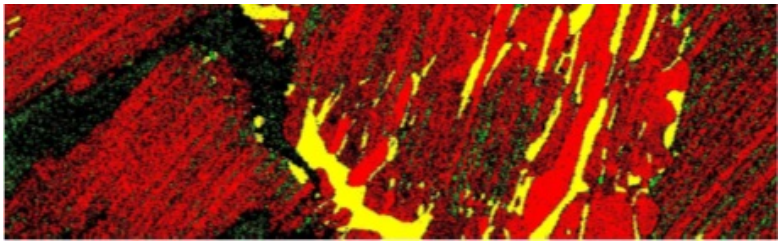

(a) around tip of sub crack

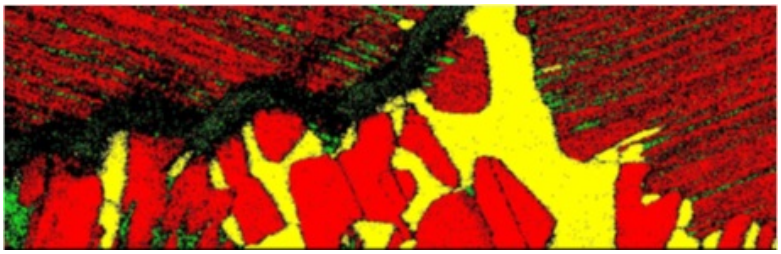

(b) around main crack

Fig. 9 Results of EBSD analysis around crack path in the NL specimen; Green: α-phase, Yellow: β-phase, Red: γ-phase.

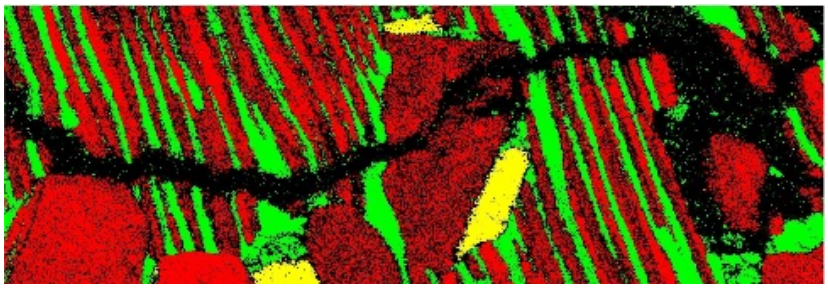

Fig. 10 Results of EBSD analysis around crack path in the TL specimen; Green: α-phase, Yellow: β-phase, Red: γ-phase.

4. Conclusions

In this work, the effect of microstructure on the fatigue crack propagation behavior under the out-of-phase type TMF condition was investigated as a part of the collaborative research. The main conclusions are summarized as follows.

(1) The fatigue crack propagated perpendicularly to the loading axis, macroscopically. However, the fatigue crack propagation behavior was strongly affected by microstructure, such as lamellar structures and grain boundaries microscopically.

(2) The fatigue crack growth resistance of the NL specimen was superior compared with the TL specimen because the driving force for crack propagation was decreased due to the branching and kinking of the main crack in the NL specimen.

(3) The crack growth rate under the out-of-phase type TMF condition was remarkably accelerated as compared with those under the iso-thermal high cycle fatigue condition.

Acknowledgment

This work was performed as a part of the collaborative research in the subcommittee on Titanium-Aluminide alloys, JSMS Committee on High Temperature Strength of Materials. The tested materials were provided by IHI. The first author (Y. Yamazaki) wish to express his gratitude to the financial support from the Amada Foundation.

References

[1] P. Janschek, Materials Today: Proceedings 2S (2015) S92 – S97

[2] B. P. Bewlay, S. Nag, A. Suzuki & M. J. Weimer, Materials at High Temperatures, 33:4-5 (2016) 549-559

[3] H. Clemens, S. Mayer, Materials at High Temperatures, 33:4-5 (2016) 560-570

[4] X. Wu, Intermetallics 14 (2006) 1114-1122

[5] H. Clemens, S. Mayer, Advanced engineering materials, 4 (2013) 15

[6] W. Wallgram, T. Schmolzer, L. Cha, G. Das, V. Giither，H. Clemens, Int. J. Mat. Res. 100 (2009) 8

[7] Y.W. Kim, S.L. Kim, JOM, 70 (2018) 4

[8] M. Thomas M.-P. Bacos, J. AerospaceLab, 3 (2011) 1-11

[9] M. Petrenec, J. Polák, J. Dluhoš, J. Tobiáš, Powder Metallurgy Progress, Vol.14 (2014) 156-162

[10] M. Filippini, S. Beretta, C. Içöz1, L. Patriarca, Mater. Res. Soc. Symp. Proc. Vol. 1 (2015) DOI:10.1557/opl.2015.32

[11] Y. Niwa, M. Sakaguchi, H. Inoue, Proc. 56th Symposium of High Temperature Strength, JSMS (2018) (in Japanese)